IEEE Access
Multidisciplinary | Rapid Review | Open Access Journal

Received October 13, 2020, accepted October 28, 2020, date of publication November 2, 2020, date of current version November 12, 2020.

Digital Object Identifier 10.1109/ACCESS.2020.3035135

Toward a Spectrally Efficient FSK Direct Antenna Modulation

JEAN PAUL DYTIOCO SANTOS[1,2], (Graduate Student Member, IEEE), KAMAL BHAKTA[1,2], FOAD FEREIDOONY[1], (Member, IEEE), AND YUANXUN ETHAN WANG[1], (Fellow, IEEE)

[1]Department of Electrical Engineering, University of California, Los Angeles, Los Angeles, CA 90095, USA
[2]Naval Air Warfare Center Weapons Division, Point Mugu, CA 93042, USA

Corresponding author: Jean Paul Dytioco Santos (jpsant2006@g.ucla.edu)

This work was supported in part by the United States Department of Defense through the Science Mathematics and Research for Transformation (SMART) Scholarship Program, and in part by the NAWCWD Independent Applied Research Program (IAR).

ABSTRACT Antennas in platforms where the physical dimensions are significantly smaller than the wavelength of the frequency of interest are limited to narrowband operations. A technique that enables transmission of such signals through narrowband antennas is called Direct Antenna Modulation (DAM). DAM utilizes switching circuitry to directly modulate the antenna at its maximum energy moments synchronized with the input RF signal. In this paper, we propose a method of attaining higher-order, N, frequency shift keyed, NFSK, modulation through a high Quality-factor electrically small antenna to achieve higher bit rates and better spectral efficiency within an instantaneous bandwidth. A DAM antenna transmitting a frequency shift keyed signal using four carrier frequencies, 4FSK, was designed, prototyped, and measured. Its electrical size is $0.018\lambda \times 0.02\lambda$. A pseudorandom 8-bit and 16-bit sequence were transmitted through the 4FSK DAM antenna and received in the far-field. The results show that such a topology provides a roadmap in attaining even higher modulation orders, thus, higher spectral efficiency.

INDEX TERMS Electrically small antennas, direct antenna modulation, time-varying electromagnetics, high-efficiency bandwidth antenna.

I. INTRODUCTION

Antennas onboard platforms which are orders of magnitude smaller than the wavelength of the desired signal are known to have narrowband performance. This limited performance is constrained by a rapid increase in the antenna's Quality factor (Q-factor) which is inversely proportional to the product of the propagation constant, k, and the radius, a, that minimally circumscribes the antenna structure [1]. Because the Q-factor is inversely proportional to the fractional bandwidth of the antenna, transmission of a high-bandwidth signal is reflected back to the source, distorted, and/or inefficiently radiated [2]. Therefore, such high-bandwidth and highly efficient radiators in electrically small-regimes are difficult to design.

However, one methodology that enables transmission of high-bandwidth signals despite this limitation is a technique known as Direct Antenna Modulation (DAM) [3]–[5]. The foundational basis in DAM is that though the high radiation Q-factor of an antenna traditionally limits the bandwidth of an electrically small antenna (ESA) with a linear time-invariant (LTI) matching circuit, the time-varying operation of an antenna may not be limited. Specifically, if the antenna is directly modulated through the use of a switching circuit, the antenna can be made to transmit amplitude shift keyed (ASK) [6]–[10], phase shift keyed (PSK) [11], [12], and frequency shift keyed (FSK) [13]–[15] signals. Earlier works [16], [17] were able to produce these high-bandwidth signals through the time-varying operation of the circuit, but an important aspect of DAM is the need to ensure synchronization between the switching action and the input RF signal so that during the transition, the maximum energy of the antenna is maintained. This was shown in [18], [19] to ensure that in the time-varying operation of DAM, maximum efficiency is attained as well as high-bandwidth transmission.

The purpose of this paper is to build on previous research and propose how to increase spectral efficiency of an FSK DAM transmitter. It is well known that out of all the binary modulation schemes, FSK requires the most bandwidth [20]. Therefore, we propose, as conventionally done, increasing the binary order of the transmission.

The associate editor coordinating the review of this manuscript and approving it for publication was Debdeep Sarkar.

Previously it was shown that the use of high figure of merit (FoM) transistors results in an FSK DAM system that capable of even greater data rates due to the increased frequency of separation between carriers [21]. However, DAM was limited to a binary modulation symbol. In this work, we further enhance the capability of DAM by creating a pathway to achieving even higher order modulations, starting with FSK. We prototyped, designed, and measured a 4FSK DAM antenna, and transmitted a pseudorandom 8-bit and 16-bit sequence and received in the far-field successfully.

The FSK DAM technique will be succinctly explained in Sec. II. In Sec. III, we propose a 4FSK DAM system and show the pathway for high order modulations and greater spectral efficiency through circuit analysis and resonator theory. Finally, far-field measurements for the 4FSK DAM in an outdoor setting will be shown in Sec. IV.

II. FREQUENCY SHIFT KEYED DIRECT ANTENNA MODULATION

A major advantage of using FSK over other digital modulation techniques is that in an FSK waveform, the signal is a constant envelope signal [20]. Specifically for DAM, the implementation for FSK experiences relatively smaller switching losses due to the change in capacitance not having to be completely either OFF or ON [7].

For an FSK DAM antenna system, the switching of the resonant frequency must be synchronized to the switching in the carrier frequency provided by the input RF signal. This ensures that maximum efficiency is attained throughout the time-varying operation of DAM. Because of this, an important choice in the design of the overall system is the antenna. In this work, we chose a capacitively loaded loop antenna (CLLA) because of its size, low manufacturing cost, and ease in matching to a 50 Ω system through a secondary loop [22]. Because the CLLA can be modeled as a simple RLC circuit with a transformer, the whole DAM system can be modeled as a circuit while including the transistors used for switching. As an example, a BFSK DAM [21] system is seen in Fig. 1.

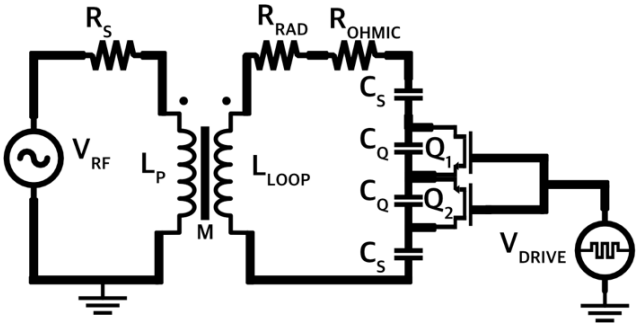

FIGURE 1. The circuit diagram of an BFSK DAM system with the transistors used to switch the resonance of the antenna.

The transistors provide a pathway for the antenna to have two resonances. When transistors Q_1 and Q_2 are both ON,

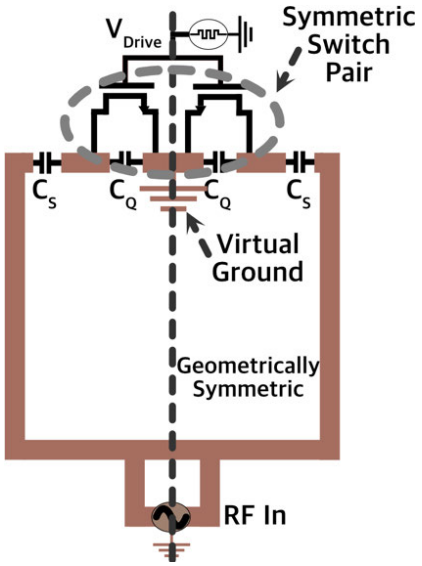

FIGURE 2. The geometry of the BFSK DAM antenna that incorporate a symmetric switch pair.

the ON-resonance is defined by:

$$f_{on} = \frac{1}{2\pi\sqrt{\frac{L_{Loop}C_s}{2}}} \tag{1}$$

where f_{on} is the resonance frequency when the transistors are ON. When the transistors are OFF, the OFF-resonance, f_{off}, is based off of an equivalent capacitance, C_{eq}, which includes the OFF-capacitance of the transistors C_{off}.

$$C_{eq} = \frac{1}{8}\frac{C_s\left(C_{off} + C_q\right)}{C_s + C_{off} + C_q} \tag{2}$$

$$f_{off} = \frac{1}{2\pi\sqrt{L_{Loop}C_{eq}}} \tag{3}$$

Therefore, if the changes in resonance of the antenna are synchronized with the input RF signal, a high efficiency bandwidth BFSK signal can be transmitted through a narrowband CLLA. Because of the requirement that the switching must occur at the moment when the antenna contains maximum energy, for a CLLA, this must occur at maximum current occurrences seen by L_{Loop}. Consequently, the switch driver signal must be made so that ON-period of V_{drive} must be an integer value of the ON-period and the OFF-period of V_{drive} must be an integer value of the OFF-period.

$$\frac{2}{f_b} = nT_{on} + mT_{off} = \frac{n}{f_{on}} + \frac{m}{f_{off}} \tag{4}$$

where f_b is the bit rate of the input signal. Now, the achieved bandwidth of the BFSK DAM, BW_{sys}, system is completely based on the bit rate, provided that the frequency separation of the two carrier frequencies are higher than the desired bit rate.

$$BW_{sys} = f_b \leq \left|f_{off} - f_{on}\right| \tag{5}$$

Theoretically, (5) shows that if the maximum efficiency is maintained through switching, the DAM system can transmit signals beyond the instantaneous impedance bandwidth of the high-Q ESA.

III. ANALYSIS AND DESIGN OF A 4FSK/N-FSK DIRECT ANTENNA MODULATION

A. TOPOLOGY TO ACHIEVE NFSK AND 4FSK DAM

A method to improve the bandwidth of the FSK DAM system, is to increase the bit rate. However, two carrier frequencies, (1) and (3), must be chosen so that their frequency difference (5) supports the chosen data rate. This ensures that the bit sequence being transmitted can be properly demodulated. However, a practical challenge here, as seen in (2) is that the transistor parasitics limit the frequency difference needed to achieve much higher data rates. Nevertheless, DAM can theoretically support data rates up to the carrier frequency [7]. Still, even if the frequency difference between the carriers is sufficient to maximize the data rate, FSK modulations are often spectrally inefficient compared to other binary digital modulation schemes [20]. Therefore, a well-known method to increase the data rates is to incorporate higher order modulation techniques. In this work, we propose a pathway to achieve N-FSK modulation. The topology is shown in Fig. 3.

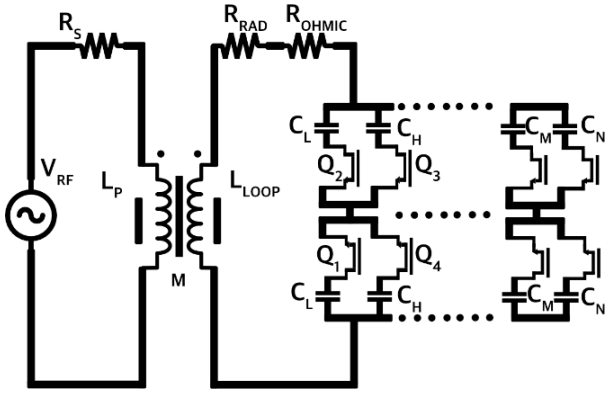

FIGURE 3. The circuit topology for an NFSK DAM system. Such a topology allows the reduction in the effect of the ON-resistance of the transistor.

To achieve isolation between the RF and switching signal, it is imperative that the RF signal in the primary side of the loop antenna sees the same reactance on both sides of the RF path. Thus, the capacitances C_L, C_H, C_M, C_N on each of the branches reside on both top and bottom of the branch. Because this symmetry produces a virtual ground, the switching signal that switches states among the parallel branches are unambiguous. This enforces the switching signal seen at the gate port of the transistor to be referenced to ground, ensuring that the transistors are switched as intended.

Therefore, to achieve 2^N bits per symbol, there must be 2N transistors. In this paper, we propose a 4FSK modulation which consists of two branches and four transistors.

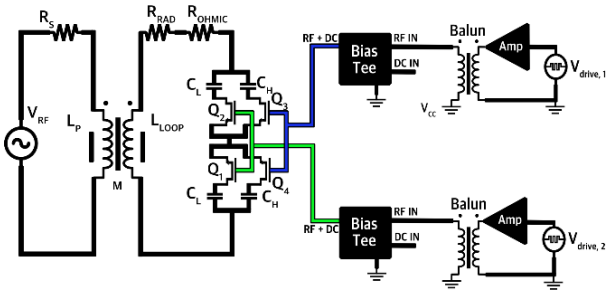

FIGURE 4. The overall circuit schematic including the driver circuitry to switch the transistors ON and OFF and the loop antenna model.

B. RESONANCE NETWORK TO ACHIEVE 4FSK DAM

The four frequencies to support a 4FSK transmission are dependent on the choice of capacitors C_L and C_H along with the parasitic capacitance of the transistor, C_{tOFF} as shown in the circuit diagram in Fig. 4. Therefore, depending on the desired carrier frequencies, C_L and C_H can be chosen considering the inherent effect of C_{tOFF}. Because of this, depending on whether the transistors are turned ON and OFF in each branch, four unique resonant states are achieved. If all the transistors are turned ON, the transistors contribute no capacitance and the resonance is wholly dependent on C_L and C_H. Specifically, the equivalent capacitance is:

$$C_{ON} = \frac{C_L + C_H}{2} \tag{6}$$

Therefore, this results in the lowest resonance frequency of:

$$f_{ON} = \frac{1}{2\pi\sqrt{L_{Loop}C_{ON}}} \tag{7}$$

Contrarily, when all transistors are OFF, each of the transistors contribute C_{tOFF}. Because of this, the equivalent capacitance in the upper left branch which contains the capacitance C_L is:

$$C_1 = \frac{C_L C_{tOFF}}{C_L + C_{tOFF}} \tag{8}$$

And the equivalent capacitance in the upper right branch which contains the capacitance C_H is:

$$C_2 = \frac{C_H C_{tOFF}}{C_H + C_{tOFF}} \tag{9}$$

Therefore, the equivalent capacitance of the whole resonance network is:

$$C_{OFF} = \frac{C_1 + C_2}{2} \tag{10}$$

Resulting in the resonance which produces the highest carrier frequency

$$f_{OFF} = \frac{1}{2\pi\sqrt{L_{Loop}C_{OFF}}} \tag{11}$$

Now, the other two resonances are achieved depending if the transistors in either left or right branches as shown in Fig. 4 are turned ON. If the left branch transistors

Q_1 and Q_2 are ON and right branch transistors Q_3 and Q_4 are OFF, the equivalent capacitance of the whole network is:

$$C_A = \frac{C_L + C_2}{2} \tag{12}$$

Similarly, if the right branch transistors Q_3 and Q_4 are ON and left branch transistors Q_1 and Q_2 are turned OFF, the equivalent capacitance of the whole network is:

$$C_B = \frac{C_1 + C_H}{2} \tag{13}$$

These result in two more distinct resonant frequencies for use in 4FSK DAM:

$$f_A = \frac{1}{2\pi\sqrt{L_{Loop}C_A}} \tag{14}$$

$$f_B = \frac{1}{2\pi\sqrt{L_{Loop}C_B}} \tag{15}$$

An advantage of this topology when compared to Fig. 1 is that the additional pair of transistors reduces the effect of the ON-resistance because of the parallel arrangement of the transistors. Therefore, by reducing the ON-resistance of the DAM system, maximum efficiency is maintained.

C. SIMULATIONS OF THE 4FSK DAM ANTENNA

To initially test the above analysis and theory, the circuit representation shown in Fig. 4 was modeled in Keysight ADS. Also, a CLLA was designed in a full-wave electromagnetic (EM) solver, Dassault Systemes CST, to capture the radiation and loss characteristics of the antenna. The CLLA combined with the switching circuitry in Fig. 4 creates the overall DAM antenna. CST simulations show that the ohmic resistance, R_{OHMIC}, is 282 mΩ while the radiation resistance, R_{RAD}, is 0.959 mΩ. When the CLLA is simulated to resonate at 35 MHz, the realized gain of the antenna is −23.56 dB. Because the CLLA is inherently a narrowband antenna, this realized gain is only achieved within the narrow impedance bandwidth, where $|S_{11}| < -10$ dB, of the CLLA.

Next, the circuit parameters attained from the EM solver were used to simulate the antenna with the switch circuitry needed to achieve the overall DAM system. $C_L = 75$ pF and $C_H = 47$ pF were chosen to create carrier frequencies around 35 MHz. Using the carrier frequencies achieved in (7), (11), (14), and (15), a 4FSK signal was generated and used as V_{RF}. The power received is computed by taking the quotient of the square of the voltage across the R_{RAD} and the resistance value of R_{RAD}. This is compared to the available power from the source. Further, to simulate the performance of CLLA, the switching circuitry was removed, resulting in only achieving the resonance frequency of (11). The simulated power spectrum achieved by both DAM and CLLA are shown in Fig. 5. As can be seen, the DAM antenna is able to follow a high bandwidth 4FSK signal by maintaining the

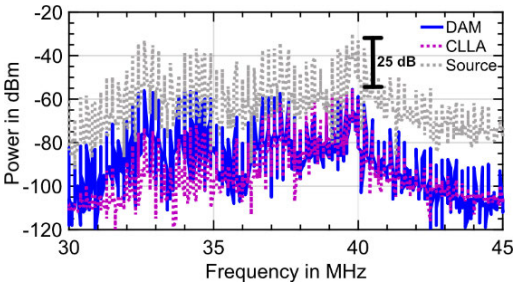

FIGURE 5. The simulated power spectrum of both the DAM and CLLA compared to an input 4FSK signal.

frequency components of the input RF signal. Quantitatively at each of the frequencies, the magnitude of DAM is such that it is approximately 25 dB below the available source power, whereas for CLLA, it is 25 dB below the available source power only at its resonance, but greatly attenuated beyond its narrow impedance bandwidth. This shows that in traditional ESA's, the frequency components outside the narrow impedance bandwidth are radiated inefficiently and are greatly attenuated.

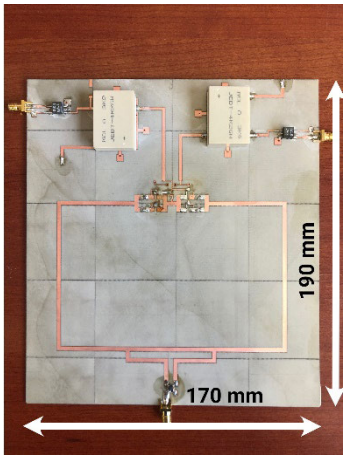

FIGURE 6. The prototype of the 4FSK HF DAM antenna including the integrated Balun and bias tee.

IV. FAR-FIELD MEASUREMENTS OF 4FSK DIRECT ANTENNA MODULATION

Next, a 4FSK DAM system was designed and prototyped centered at 35 MHz. The prototyped antenna is shown in Fig. 6 using capacitor values $C_L = 75$ pF and $C_H = 47$ pF. At f_{ON}, its electrical size is 0.018λ by 0.02λ (170 mm × 190 mm). To further enhance the isolation of the 4FSK DAM antenna, a balun, DA2319-ALB, was integrated into the switching circuitry as well as an integrated bias tee, Mini Circuits JEBT-4R2GW. A Tektronix AWG 5208 was used to generate the switching signal. For this design, a EPC 2036 transistor [23] was used since it has a higher FoM that will yield an increased frequency difference

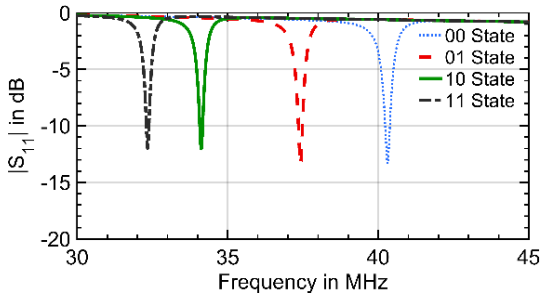

FIGURE 7. The $|S_{11}|$ performance of the 4FSK DAM antenna.

between f_{max} and f_{min}. The EPC 2036 transistor contains $C_{tOFF} = 165$ pF. Because of the circuit topology in Fig. 4, the effective switching resistance by the transistor is $R_{tON} = 73$ mΩ. To ensure that the transistors are effectively switched ON and OFF, the switching signal was externally amplified using a 24 dB Mini Circuits ZHL-3A+ to produce an 8 V_{pp} switching signal. It is critical to bias the transistor with sufficient V_{GS} as possible during the ON-state due to the different slopes of the IV curve given V_{GS} [23]. With a high V_{GS}, a lower ON-resistance is experienced. Another important note is that each switching signal biases a branch so that at any given state, the impedance seen by the RF signal is the same on both sides geometrically, retaining symmetry. This assists in isolating both the RF and switching signals from each other. To ensure that at each resonance state that DAM system achieves maximum efficiency, the $|S_{11}|$ performance of the 4FSK DAM was measured to determine the four carrier frequencies. It is assumed that the during these switching states, the capacitance contributed by the transistor is 0, due to a low R_{tON}, and only contributes capacitance during the OFF-state through C_{tOFF}. These are shown in Fig. 7. Based on this measurement, the carrier frequencies to support 4FSK are well-matched to a 50 Ω source ($|S_{11}| < -10$ dB) and should maximize the efficiency of the 4FSK DAM antenna.

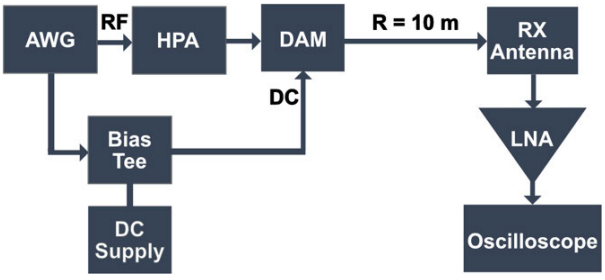

FIGURE 8. The far-field measurement schematic of the 4FSK DAM system.

Next, the far-field measurement setup for the 4FSK DAM is shown in Fig. 8. The transmitter and receiver were separated by at least one wavelength away to achieve far-field radiation recommended in [24]. A 2.5% modulation rate 4FSK signal was transmitted, and a pseudorandom 8-bit and 16-bit sequence was encoded using the four resonances attained in the 4FSK DAM antenna. The four transistors can be turned OFF and ON in a pattern to achieve four distinct resonant frequencies. Therefore, to properly encode a bit sequence, the carrier frequencies are encoded with a binary digit. These are shown in Table 1. Therefore, the bit sequence "11-01-00-10" and "11-01-10-00-01-11-00-10" was transmitted for the 8-bit and 16-bit sequence respectively at a rate of 1.79 Mbps and RF input power of 15 dBm. Because the EPC2036 transistor has a C_{gs} of 89 pF, the drive power used to turn ON and OFF the transistors is calculated to be 1.3 mW, at a bit rate of 1.79 Mbps.

TABLE 1. Resonance frequency to binary digit in 4FSK DAM.

Resonance Frequency	Binary	$V_{drive,1}$	$V_{drive,2}$
32.32 MHz	11	HIGH	HIGH
34.12 MHz	10	HIGH	LOW
37.44 MHz	01	LOW	HIGH
40.36 MHz	00	LOW	LOW

To show the ability of the 4FSK DAM system in transmitting signals beyond its instantaneous impedance bandwidth, the time-domain and frequency-domain signal were received using an oscilloscope, Tektronix MSO-64. Furthermore, to ensure that the 4FSK DAM antenna works as intended, the same bit sequence was transmitted but the switching signal was turned OFF to compare the 4FSK DAM antenna to another conventional electrically small antenna such as a CLLA without DAM that is only resonant at one of the carrier frequencies, 40 MHz. Its $|S_{11}|$ performance is shown in Fig. 7 shown by the "00-State" since without the switching circuitry, the DAM antenna devolves to a traditional CLLA. In this way, a comparison is made to show how a conventional high-Q ESA cannot adequately transmit high-bandwidth signals such as 4FSK. The spectrogram results are shown in Fig. 9 and the frequency-domain results are shown in Fig. 10.

In Fig. 10, the 4FSK DAM antenna can retain the signal's spectrum far more capably than a CLLA. Since the CLLA is solely resonant at around 40 MHz due to the absence of the switching mechanism in DAM, the received spectrum, when compared to DAM is comparable at this center frequency. But because CLLA does not have the switching inherent in DAM, it cannot transmit the other tones well. Quantitatively, without synchronization between the RF and switching signals, the spectral efficiency of a CLLA diminishes significantly. Yet, with DAM, for both 8-bit and 16-bit transmissions, the spectrum is mostly maintained. The spectrogram in Fig. 9 also further illustrate the effectiveness of DAM. Fig. 9 shows that for both 8-bit and 16-bit patterns, the 4FSK DAM antenna was able to transmit and distinguish the bit patterns whereas for the CLLA, the bit sequence is hardly observable.

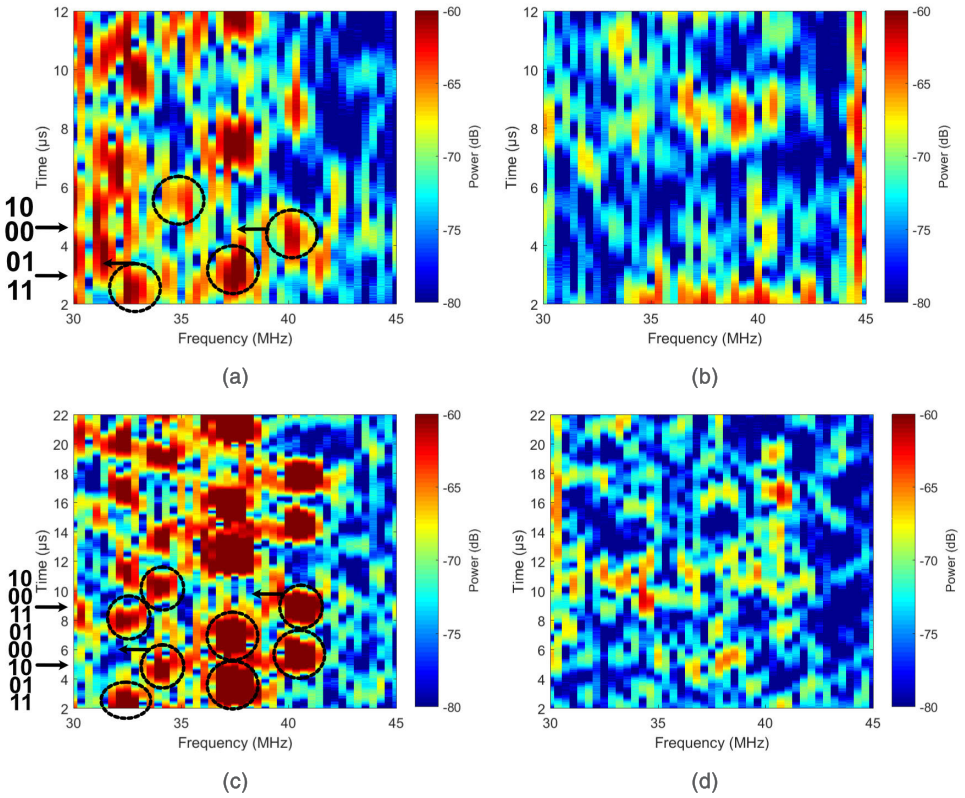

FIGURE 9. The spectrogram for the received signal from the 4FSK DAM antenna (a) (c) and CLLA (b) (d) for the 8-bit (top) and 16-bit (bottom) sequence.

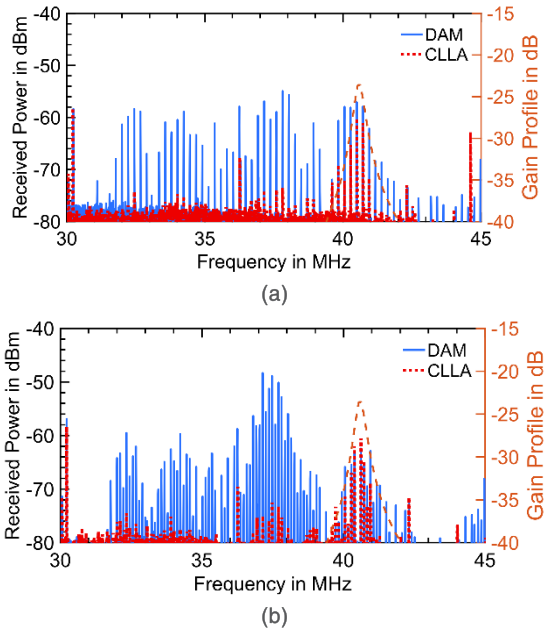

FIGURE 10. The received spectrum from the 4FSK DAM antenna (blue) and CLLA (red) transmitting an 8-bit (a) and 16-bit sequence (b). The antenna gain (orange) at one of its resonance is included.

A quantitative and useful way to evaluate the performance of the antennas is through a figure of merit called efficiency-bandwidth (EB) product. This measures the radiation efficiency along with the instantaneous bandwidth of the antenna [25]. Specifically, a way to quantify the improvement of the DAM antenna in comparison with the CLLA called $\beta_{measured}$ [21] which compares the EB of both antennas

$$\beta_{measured} = \frac{EB_{DAM}}{EB_{CLLA}} = \frac{e_{DAM}}{e_{CLLA}} \frac{BW_{DAM}}{BW_{CLLA}} \tag{16}$$

where EB_{DAM} and EB_{CLLA} is the EB of the DAM and CLLA, respectively. The efficiencies, e_{DAM} and e_{CLLA} can be calculated by the ratio of the sum of the received tones, shown in Fig. 10, and the sum of the transmitted tones. BW_{DAM} is calculated using (5) and BW_{CLLA} is calculated where the $|S_{11}| \leq -7$ dB. Through (16), the measured EB improvement of DAM over CLLA, $\beta_{measured}$, is 4.66.

Although there is an improvement of DAM over CLLA, various nonidealities and practical issues may affect the achieved $\beta_{measured}$ due to the decrease in efficiency. An issue that arises is the effect of Joule heating. This practical issue leads to an even higher switching resistance. However, because the effective switching resistance is only $R_{tON} = 73$ mΩ, which is about 25% of the antenna ohmic resistance, $R_{OHMIC} = 282$ mΩ, the effect of Joule heating is minimal. Another critical important design methodology is to ensure that the switching occurs at moments when the current in the loop antenna is maximum. A practical error that occurs if the needed precision to maintain this switching condition is

not held. Moreover, non-idealities from to the transient characteristics of the driver circuitry add to these errors. These then result in lower achieved efficiency for DAM. To enhance the precision, a higher sampling rate waveform generator can be used to generate the switching signal synchronous to the input RF signal. This is tremendously important especially for even higher-order FSK modulations due to the increase in switching rates that lead to higher switching losses, and thus, lower overall efficiencies.

V. CONCLUSION

In this paper, we provided a pathway to achieve a more spectrally efficient DAM transmitter. This is achieved using a geometrically symmetrical antenna topology and higher order modulations, respectively. In a 4FSK DAM system, the use of parallel branches with N transistors for 2^N bits per symbol, combined with a higher FoM transistor, enables even higher spectral efficiency compared to binary digital modulation techniques. The far-field measurements show significant improvement over a conventional ESA such as a CLLA.

The 4FSK DAM design in this work is more much more spectrally efficient because the modulation scheme achieves twice the number of bits per symbol compared to the BFSK DAM design. This results in higher bit rates.

Another important aspect is that with a 4FSK DAM design, the physical size increases to support two switching waveforms. This is due to the addition of the balun and integration of the bias tee directly into the PCB. Increasing the physical size aids in boosting the antenna gain due to the increase of aperture area.

The topology and technique here provide a pathway for other DAM methodologies to achieve higher spectral efficiency through N-order bit transmissions. Through even better FoM transistors, even higher bit rates can be achieved.

ACKNOWLEDGMENT

The authors would like to thank Dr. D. Mensa from the Naval Air Warfare Center Weapons Division, Point Mugu, CA, USA, for his detailed review and suggestions for the work. Distribution Statement A: Approved for public release; distribution is unlimited. NAWCWD PR20-0089. The views expressed are those of the authors and do not reflect the position or policy of the U.S. Department of Defense.

REFERENCES

[1] L. J. Chu, "Physical limitations of omni–directional antennas," *J. Appl. Phys.*, vol. 19, no. 12, pp. 1163–1175, Dec. 1948, doi: 10.1063/1.1715038.

[2] R. M. Fano, "Theoretical limitations on the broadband matching of arbitrary impedances," *J. Franklin Inst.*, vol. 249, no. 1, pp. 57–83, Jan. 1950, doi: 10.1016/0016-0032(50)90006-8.

[3] M. Manteghi, "Fundamental limits, bandwidth, and information rate of electrically small antennas: Increasing the throughput of an antenna without violating the thermodynamic Q-Factor," *IEEE Antennas Propag. Mag.*, vol. 61, no. 3, pp. 14–26, Jun. 2019, doi: 10.1109/MAP.2019.2907892.

[4] J. P. Santos, F. Fereidoony, M. Hedayati, and Y. E. Wang, "High efficiency bandwidth electrically small antennas for compact wireless communication systems," in *IEEE MTT-S Int. Microw. Symp. Dig.*, Jun. 2019, pp. 83–86.

[5] K. Schab, D. Huang, and J. J. Adams, "Pulse characteristics of a direct antenna modulation transmitter," *IEEE Access*, vol. 7, pp. 30213–30219, 2019, doi: 10.1109/ACCESS.2019.2902365.

[6] M. I. Jacob and H. N. Brauch, "Keying VLF transmitters at high speed," *Electronics*, vol. 27, no. 12, pp. 148–151, 1954.

[7] U. Azad and Y. E. Wang, "Direct antenna modulation (DAM) for enhanced capacity performance of near-field communication (NFC) link," *IEEE Trans. Circuits Syst. I, Reg. Papers*, vol. 61, no. 3, pp. 902–910, Mar. 2014, doi: 10.1109/TCSI.2013.2283995.

[8] S. Srivastava and J. J. Adams, "Analysis of a direct antenna modulation transmitter for wideband OOK with a narrowband antenna," *IEEE Trans. Antennas Propag.*, vol. 65, no. 10, pp. 4971–4979, Oct. 2017, doi: 10.1109/TAP.2017.2734063.

[9] X. Xu and Y. Ethan Wang, "Beyond the efficiency bandwidth limit with switched electrically small antennas," in *Proc. IEEE Antennas Propag. Soc. Int. Symp.*, Jun. 2007, pp. 2261–2264, doi: 10.1109/APS.2007.4395981.

[10] M. Manteghi, "A wideband electrically small transient-state antenna," *IEEE Trans. Antennas Propag.*, vol. 64, no. 4, pp. 1201–1208, Apr. 2016, doi: 10.1109/TAP.2016.2525828.

[11] R. Zhu and Y. E. Wang, "A modified QPSK modulation technique for direct antenna modulation (DAM) systems," in *Proc. IEEE Antennas Propag. Soc. AP-S Int. Symp.*, 2014, pp. 1592–1593, doi: 10.1109/APS.2014.6905122.

[12] K. Schab, D. Huang, and J. J. Adams, "An energy-synchronous direct antenna modulation method for phase shift keying," *IEEE Open J. Antennas Propag.*, vol. 1, pp. 41–46, Oct. 2020, doi: 10.1109/ojap.2020.2972842.

[13] M. Salehi, M. Manteghi, S.-Y. Suh, S. Sajuyigbe, and H. G. Skinner, "A wideband frequency-shift keying modulation technique using transient state of a small antenna," *Prog. Electromagn. Res.*, vol. 143, pp. 421–445, 2013.

[14] R. Zhu, S. P. Selvin, Y. E. Wang, and N. Guo, "Frequency shift keying for Direct Antenna Modulation (DAM) with electrically small antenna," in *Proc. IEEE Antennas Propag. Soc. Int. Symp. Process.*, Jan. 2017, pp. 1203–1204, doi: 10.1109/APUSNCURSINRSM.2017.8072644.

[15] J. P. Santos, F. Fereidoony, and Y. E. Wang, "Enabling high efficiency bandwidth electrically small antennas through direct antenna modulation," in *Proc. IEEE Int. Symp. Antennas Propag. Usn. Radio Sci. Meet.*, Dec. 2019, pp. 1539–1540, doi: 10.1109/APUSNCURSINRSM.2019.8889265.

[16] H. Wolff, "High-speed frequency-shift keying of LF and VLF radio circuits," *IEEE Trans. Commun.*, vol. 5, no. 3, pp. 29–42, Dec. 1957, doi: 10.1109/TCOM.1957.1097513.

[17] H. Hartley, "Analysis of some techniques used in modern LF-VLF radiation systems," *IEEE Trans. Commun.*, vol. 16, no. 5, pp. 690–700, Oct. 1968.

[18] J. Galejs, "Switching of reactive elements in High-Q antennas," *IEEE Trans. Commun. Syst.*, vol. 11, no. 2, pp. 254–255, Jun. 1963, doi: 10.1109/tcom.1963.1088740.

[19] J. Galejs, "Electronic broadbanding of high-Q tuned circuits or antennas," *Arch. Elek. Ubertragung*, vol. 17, no. 8, pp. 375–380, 1963.

[20] B. P. Lathi and Z. Ding, *Modern Digital and Analog Communication Systems*, 4th ed. London, U.K.: Oxford Univ. Press, 2009.

[21] J. P. D. Santos, F. Fereidoony, M. Hedayati, and Y. E. Wang, "High efficiency bandwidth VHF electrically small antennas through direct antenna modulation," *IEEE Trans. Microw. Theory Techn.*, early access, Aug. 25, 2020, doi: 10.1109/TMTT.2020.3016381.

[22] J. van Niekerk, "Matching Small Loop Antennas to rfPIC TM Devices," *Microchip Technol.*, vol. 15, pp. 1–8, Dec. 2002.

[23] *EPC2036—Enhancement Mode Power Transistor*, EPC, El Segundo, CA, USA, 2009. [Online]. Available: https://epc-co.com/epc/Products/eGaNFETsandICs/EPC2036.aspx

[24] W. L. Stutzman and G. A. Thiele, *Antenna Theory and Design*, 3rd ed. Hoboken, NJ, USA: Wiley, 2012.

[25] D. F. Sievenpiper, D. C. Dawson, M. M. Jacob, T. Kanar, S. Kim, J. Long, and R. G. Quarfoth, "Experimental validation of performance limits and design guidelines for small antennas," *IEEE Trans. Antennas Propag.*, vol. 60, no. 1, pp. 8–19, Jan. 2012, doi: 10.1109/tap.2011.2167938.

JEAN PAUL DYTIOCO SANTOS (Graduate Student Member, IEEE) received the B.S. degree *(summa cum laude)* in electrical engineering from The University of Utah (UofU), Salt Lake City, UT, USA, in 2013, and the M.S. degree in electrical engineering from the University of California, Los Angeles (UCLA), Los Angeles, CA, USA, in 2015. He is currently pursuing the Ph.D. degree with the Digital Microwave Laboratory under Prof. Y. E. Wang.

He is also an RF Engineer with the Naval Air Warfare Center Weapons Division (NAWCWD), Point Mugu, CA USA. While at UCLA, he was involved with the Antenna Research, Analysis, and Measurement (ARAM) Laboratory and conducted research in antenna arrays, feed networks, and broadband patch antennas. His research interests include time-varying electromagnetics, electrically small antennas, wireless communication systems, and radar. He is also a member of Tau Beta Pi. He also received several awards and is actively involved with student and professional groups. At the University of Utah, he was awarded both the Outstanding Senior Thesis Individual Presentation and Outstanding Electrical Engineering Student Award. During his time at UCLA, he was awarded the Eugene Cota V. Robles Fellowship, Tau Beta Pi Lynnworth Fellowship, as well as the prestigious Science for Mathematics and Research for Transformation Fellowship (SMART) from the Department of Defense. He was also the inaugural champion of the 2015 UCLA Graduate School Grad Slam Masters and Doctoral Research Showcase, and a recipient of the Distinguished Master's Thesis Award in Physical and Wave Electronics as well as the UCLA Edward K. Rice Outstanding Master's Student. In 2015, he was a student paper competition finalist in the 2015 IEEE Antennas and Propagation Society Conference for his research in antenna arrays for Direct-to-Earth communications in Mars rovers.

KAMAL BHAKTA received the B.E. and M.E. degrees in electrical engineering from the Stevens Institute of Technology, Hoboken, NJ, USA, in 2014, and the Ph.D. degree from the Digital Microwave Laboratory, UCLA, in 2019, under Prof. Y. Wang. He is currently an RF Instrumentation Design Engineer with the Naval Air Warfare Center Weapons Division (NAWCWD), Point Mugu, CA, USA. His research interests include smart antenna systems, telemetry, and time-varying electromagnetics. He was recognized as one of the top naval innovators by SECNAV in 2015 for strain sensor embedding within additively manufactured parts and was awarded the Science for Mathematics and Research Transformation Fellowship from the DoD in 2019.

FOAD FEREIDOONY (Member, IEEE) received the Ph.D. degree in electrical engineering from the K. N. Toosi University of Technology (KNTU), Tehran, Iran, in 2017. He is currently pursuing his research at UCLA on signal processing and design of systems for localization purposes. He was a Visiting Scholar with the University of California, Irvine (UCI), in 2016. He has been a Postdoctoral Researcher with UCLA since 2017. His research interests include applied electromagnetics, antennas, RF systems, and signal processing.

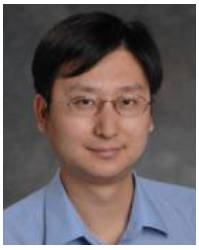

YUANXUN ETHAN WANG (Fellow, IEEE) received the B.S. degree in electrical engineering from the University of Science and Technology of China (USTC), Hefei, China, in 1993, and the M.S. and Ph.D. degrees in electrical engineering from The University of Texas at Austin, in 1996 and 1999, respectively.

He became an Assistant Professor at the Department of Electrical and Computer Engineering, UCLA, in November 2002. He is currently a Full Professor with the Department of Electrical and Computer Engineering. He is also the Director of the Digital Microwave Laboratory and the Center for High Frequency Electronics, Department of Electrical and Computer Engineering, UCLA. He has published more than 200 journal and conference papers. His research interest includes microwave systems. His expertise ranges from system to devices. His researches blend digital technologies and concepts into RF design, which often leads to novel devices with performances beyond the conventional bound. He is also an IEEE Fellow with the Microwave Theory and Techniques (MTT) Society. He was a co-recipient of the first place Best Student Paper in 2017 International Microwave Symposium and the Best Student Paper Award in 2017 GOMAC Tech Symposium. He has served as an Associate Editor for IEEE TRANSACTIONS ON ANTENNAS AND PROPAGATION.